Moroccan Journal of Chemistry
ISSN: 2351-812X
http://revues.imist.ma/?journal=morjchem&page=login
Mrharrab & al. / Mor. J. Chem. 9 N°4 (2021) 628-638
DOI: https://doi.org/10.48317/IMIST.PRSM/morjchem-v9i4.27263

Effect of starting materials on the structure of pure and Gd-doped $BaTiO_3$ elaborated by the sol gel process

L. Mrharrab[(a)], A. Nfissi[(b)], Y. Ababou[(b)*], M. Belhajji[(b)], S. Sayouri[(b)], A. Faik[(c)]

[(a)] *ERMAM, Department of physics-chemistry, FPO, B.P. 638, Ouarzazate, Morocco*
[(b)] *LPAIS, Department of physics, FSDM, USMBA, B.P. 1796, Fez, Morocco*
[(c)] *MSN Department, University Mohammed VI Polytechnic, Ben Guerir, Morocco*

** Corresponding author:*
yahya.ababou@usmba.ac.ma
Received 04 July 2020 ,
Revised 04 Dec 2021 ,
Accepted 05 Dec 2021

Abstract

Undoped and Gd-doped $BaTiO_3$ samples, with the chemical formula $BaGd_xTi_{1-x}O_{3-x/2}\square_{x/2}$, x = 0.00; 0.01; 0.02; 0.03; 0.04 and 0.05, were synthesized using the sol gel process. During the procedure of preparation of these samples acetic acid and distilled water were used as solvents. All the powders corresponding to the two series of undoped and doped samples were calcined in air at different temperatures and their crystalline phase was checked using results from XRD and Raman analyses. Acetic acid was shown to provoke the formation of the stable pseudo cubic structure for the two series of samples at relatively low temperature of crystallization, while with the use of distilled water only (without acetic acid) the tetragonal phase prevailed. In this study, the effect of acetic acid is discussed and the latter seems to play a more or less important role in the formation of the structure of BT material.

Keywords: *Barium titanate, sol gel process, crystalline structure, XRD, Raman analysis.*

1. Introduction

Piezoelectric materials have a great importance in the current industry, especially, in ultrasound, medicine or in velocimetry. Ferroelectric materials are widely used as dielectrics, capacitors, electromechanical converters, infrared detectors, memories, microwave, etc. Among these materials, the family of perovskites, of general formula ABO_3, has the advantage of modifying their physical properties under external constraints, for example by the very numerous possibilities of substitution of cations A and B, which allows a large study for this type of materials [1- 4]. Barium titanate $BaTiO_3$ (BT), a piezoelectric and dielectric material with a perovskite structure, has been extensively investigated for ferroelectric and piezoelectric properties, and was widely applied in electronic industries, especially in the multilayer ceramic capacitors (MLCC) due to its high dielectric constant and low loss [5]. Some researchers reported results of their investigations of the correlation between grain-size and the lattice structure of barium titanate ceramics prepared by the sol-gel method [6]. Other works have focused on the effect of substitution of Ba and/or Ti atoms by different chemical elements in BT matrix on dielectric characteristics of the latter [7-10], such as increasing the permittivity of the material or lowering of its transition temperature [4,11]. Also, in the context of materials intended for microelectronics, the trend towards miniaturization has directed research towards the development of organic-inorganic composites and of nanocomposites[12-14]. So, some authors have worked on composites based on polymers and barium titanate [15]. Some works have invoked the possibility of stabilizing the pseudo cubic structure under certain chemical conditions of elaboration of BT [16-18]. The aim of the present work is to study the possible effect of acetic acid on the crystalline structure of BT in comparison to the same effect but with the use of distilled water (without any acetic acid) during the process of elaboration of the material. Moreover, we have studied the effect of substitution of Ti atoms by Gd ones, in conformity with the chemical formula: $BaGd_xTi_{(1-x)}O_{(3-x/2)}\square_{(x/2)}$, on the crystalline properties of BT.

2. Experimental procedure

2.1. ***Samples preparation***

Samples of undoped $BaTiO_3$ were prepared using the sol-gel process. First, the titanium isopropoxide (99% purity, Aldrich) was dissolved in an aqueous solution of lactic acid to obtain a colloidal solution of titanium called S1. Acetic acid was then added to an adequate amount of Barium acetate (99% purity, Aldrich) dissolved in a solution of distilled water (Solution S2). The mixture (S1 + S2) was put under agitation in 60 °C for 30 min, and then dried at 80 °C for approximately three days. Xerogels of BT were grounded in a mortar during 1h. Thermal treatments were carried out by heating the dried products in air at 2 °C/min to various temperatures from 600 to 1000 °C, and holding these temperatures constants for 8h or (4h) before furnace cooling. The obtained powders were grounded another time in a mortar during 30 min. In a second step, other samples of undoped BT were synthesized by the sol-gel process except that we didn't add acetic acid to the solution of Ba. All the powders were structurally characterized by X-ray diffraction and by Raman spectroscopy. Gd-doped $BaTiO_3$ (called BGT) samples were elaborated using the sol-gel method according to the formula $BaGd_xTi_{1-x}O_{3-x/2}\square_{x/2}$(x = 0.00, 0.01, 0.02, 0.03, 0.04 and 0.05). The starting materials were Titanium isopropoxide (99% purity, Aldrich), the gadolinium acetate (99% purity, Aldrich), Barium acetate (99% purity, Aldrich), lactic acid and acetic acid as solvents. We used the colloidal solution of titanium as the source of Ti. A stoichiometric amount of the sol of Titanium was added to the gadolinium acetate dissolved in distilled water plus acetic acid or in distilled water. Then, the barium acetate dissolved in distilled water plus acetic acid or in distilled water was added to this solution. In each case (without or with acetic acid) a stirring was performed at 60 °C for 30 min followed by a drying at 80 °C for approximately three days. Thermal treatments were carried out by heating the

dried products in air to various temperatures from 600 to 1050 °C, with holding these temperatures constants for 8h or (4h) before furnace cooling.

2.2. Characterization equipment

The thermo gravimetric analysis was used to determine the temperature of crystallization of BT and BGT powders and their crystal structures were determined by X-ray diffraction (Diffractometer system = XPERT-PRO) using a CuKα radiation (λ=1.54059 Å), and a Raman spectrometer (SENTERRA).

3. Results and discussion

3.1. Part 1: Elaboration of BT and BGT samples with acetic acid as solvent

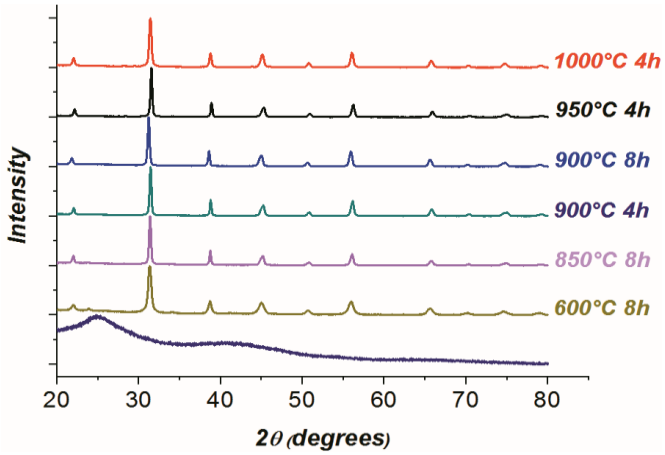

Figure 1. XRD patterns of $BaTiO_3$ powders calcined at different temperatures

In order to investigate the temperature effect on the crystalline phase of the as-prepared $BaTiO_3$ powder, samples of the latter were calcined at different temperatures. Fig.1 shows the XRD patterns of the $BaTiO_3$ powders calcined at 600 °C for 8h, 850 °C for 8h, 900 °C for 4h, 900°C for 8h, 950 °C for 4h and 1000 °C for 4h. The $BaTiO_3$ Xerogel started to crystallize at 600 °C with a secondary phase of $BaCO_3$ (peak around 24°). The barium carbonate impurity phase disappeared for the sample calcined at 850 °C, and the corresponding pattern (Fig. 1) showed a fully crystallized pseudo cubic perovskite structure, as no peak splitting indicating the presence of the tetragonal phase was observed. When the samples were calcined at higher temperatures: 900 °C (4h), 900 °C (8h), 950 °C (4h) and 1000 °C (4h), the corresponding patterns still did not show any splitting of the peaks in favor of the tetragonal phase. This indicates that, in the temperature interval considered, the $BaTiO_3$ has a very stable pseudo cubic structure. A stable cubic structure was reported for $BaTiO_3$ prepared by a chocolate acetate sol-gel process [17]. According to the authors of Ref. 17, acetic acid was added to barium acetate and titanium bis(ammonium lacto) dihydroxide was used as precursor, and the stability of the cubic phase was explained as due to the existence of a critical crystallite size giving rise to the tetragonal to cubic phase transition, that is to say that if the crystalline size is less than the critical grain size, the phase should be cubic [17,19]. It is also believed that the critical grain size may vary depending on the nature of the starting materials and synthesis process. Wei Li and al. [18] have synthesized $BaTiO_3$ nanopowders from alkoxide solution precursor by the sol gel process. They used tetrabutyl titanate, absolute ethanol and glacial acetic acid for the sol of Ti and they used barium acetate and acetic acid in Ba aqueous solution. They obtained a cubic structure, and the average crystallite size of the powders calcined at 800 °C, calculated with the help of the Scherrer's equation was 39 nm. The average crystallite size of our $BaTiO_3$ powders calcined at 1000 °C and also estimated by the Scherrer's equation is

around 37 nm. In fact, the existence of the cubic BT at room temperature has been reported to be affected by several factors, such as calcination temperature, starting materials used for precipitation, precipitates obtained and the crystallite size. We can exclude the crystallite size from these reasons because other works [11] have obtained a quadratic phase with an ultrafine BT powder (crystallite size around 23 nm). As we have worked in the high temperature region, we can also exclude the effect of the calcination temperature. In our samples, the pseudo cubic structure was probably achieved due to the starting materials used for precipitation or to the precipitates obtained. To give a better illustration of the crystalline phase of our samples, Raman spectroscopy was employed to investigate the structure of the powders and to confirm the XRD results. It is known that Raman spectroscopy may be used to study the expected structural phase transition. This technique is employed to observe vibrational, rotational and other low frequency modes in a system. The graphs (Fig.2) show the characteristic Raman peaks at room temperature of $BaTiO_3$ calcined at different temperatures.

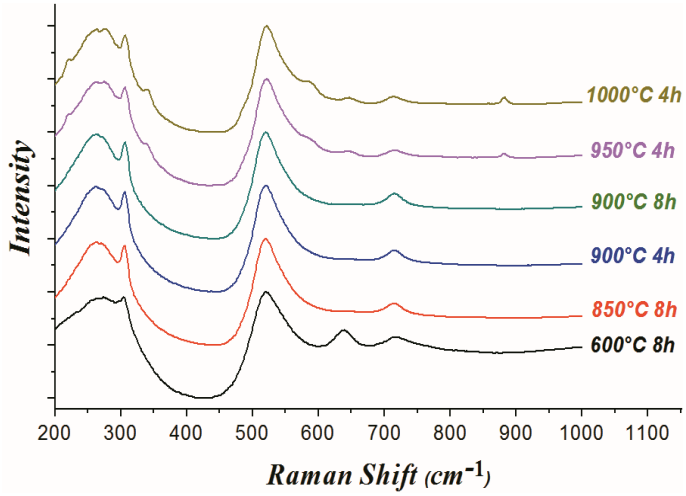

Figure 1. Room temperature Raman spectroscopy for $BaTiO_3$ powders calcined at different temperatures

We can observe from these patterns, that all the BT samples show a similar behavior (similar spectrum) except for the mode at 306 cm^{-1} which intensity changes by increasing the temperature. The Raman modes are [A1(LO)] mode at 184 cm^{-1}; [A1(TO)] mode at 279 cm^{-1}; a sharp peak associated with [B1, E(LO,TO)] mode at 306 cm^{-1}, [A1(TO3)] mode at 518 cm^{-1}; [A1(LO3), E(LO)] mode at 712 cm^{-1}. Although the cubic phase theoretically does not reveal any Raman active modes, Raman analysis generally shows broad bands at around 250 cm^{-1} and 520 cm^{-1}, which may be caused by local disorder, associated with the position of Ti atoms [20]. In the same context, a large number of researchers agree on the fact that the presence of the mode around 305 cm^{-1}, which comes from the inactive F2u mode of the cubic phase, is a characteristic of the tetragonal phase of BT [11]. Consequently, the first view of the spectrum gives us the impression that the phase is quadratic but the modes are large compared to the modes observed in the quadratic phase of BT published in several works [11, 20-21]. Because of this, for our BT samples, the Raman spectra show a crystal phase of very low quadracity very close to the pseudo-cubic structure. In Table 1 we have indicated the intensity of the [B1, E(LO,TO)] modes in BT samples as a function of temperature. We notice an increase in the intensity of [B1, E(LO,TO)] mode followed by a decrease then another increase. On the other hand, we notice a low modification in the frequencies of the Raman modes.

Table 1. ***Intensity of [B1, E(LO,TO)] mode as function of temperature***

Temperature	600°C 8h	850°C 8h	900°C 4h	900°C 8h	950°C 4h	1000°C 4h
Intensity	8684,23	22884,29	29197,89	17344,99	17503,77	20162,43

Moreover, we have examined the influence of incorporation of low concentrations of Gadolinium on the structure of BT powders elaborated by the sol gel method. We have adopted the chemical formula: $BaGd_xTi_{(1-x)}O_{(3-x/2)}\square_{(x/2)}$(BGTx). These samples were synthesized following the same procedure as for the BT ones. Fig.3 shows the thermogravimetric (TG) curves of BGT5% powder. This analysis can identify the different reactions that can be observed during the calcination process, and may provide the value of the temperature of crystallization of the sample. The TG spectrum of Fig.3 shows the thermal analysis performed until 1000 °C. We can observe an overall weight loss of about 40%. At 650 °C, the weight loss becomes weak, so we can explain it by the formation of the oxide from this temperature. Beyond 850 °C, the weight loss becomes approximately constant by increasing the temperature. This result from the TG spectrum agrees with those of XRD patterns shown in Fig.1 which indicates the formation of the oxide at the temperature 600 °C.

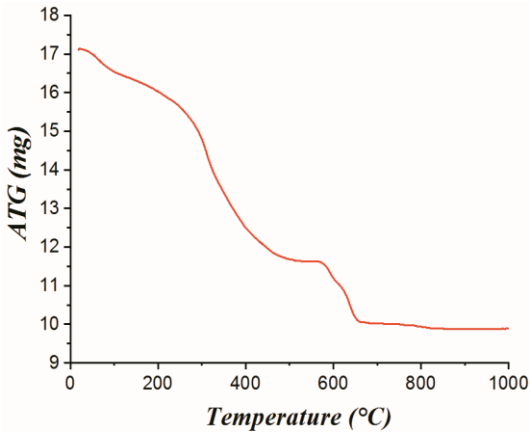

Figure 3. TG Spectrum of BGT5%

Fig.4 shows the XRD patterns of the Gadolinium doped BT powders, from 1% to 5% of Gd, calcined at 950 °C for 4h. We have chosen this calcination temperature because the TG curves show a very high stability from 900 °C. As shown in Fig.4, the BGT powders still demonstrate the presence of the pseudo cubic structure with a secondary phase (the peak 2θ~24). As mentioned in the literature [22] the gadolinium only causes the transition to the pseudo-cubic phase for concentrations greater than 30%. From this, we can conclude that the pseudo-cubic phase observed in our samples is not influenced by the doping element used. However, this element has a noticeable effect on the size of crystallites (Table.2). Table 2 gathers the values of the average crystallite size, the position of the (111)-Peak and volume of lattice. From these results, we can have an idea on the site occupied by the atoms of Gd. As seen from Table 2, a shifting to the left of the position of the peak (111) is observed until x = 0.02, accompanied by an increase of the cell volume followed by a shifting to the right for x > 0.03. This behavior can be explained as due to the incorporation of Gd of both Ba and Ti sites with predominance of occupation of Ti sites for $x \leq 0.02$ and vice versa as the ionic radii, R, of Gd, Ti and Ba are such as $R_{Ti} < R_{Gd} < R_{Ba}$. Some studies have revealed the incorporation of chemical elements in both A and B sites in the perovskite structure [23].

Table 2. ***The average crystallite size; the position of the (111)-Peak; lattice parameters (a, c) and lattice volume of BGT samples***

Samples	a. c. s. (nm)	p. of the (111)-Peak	a (Å)	c(Å)	c-a(Å)	V(Å^3)
0%	38.89	31.52436	3.990	4.000	0.010	63.9680
1%	35.02	31.49036	3.999	4.000	0.010	63.9680
2%	31.06	31.35436	4.000	4.010	0.010	64.1600
3%	31.13	31.54136	3.999	4.000	0.001	63.9680
4%	29.73	31.52436	4.000	4.010	0.010	64.1600
5%	30.01	31.52436	3.999	4.000	0.001	63.9680

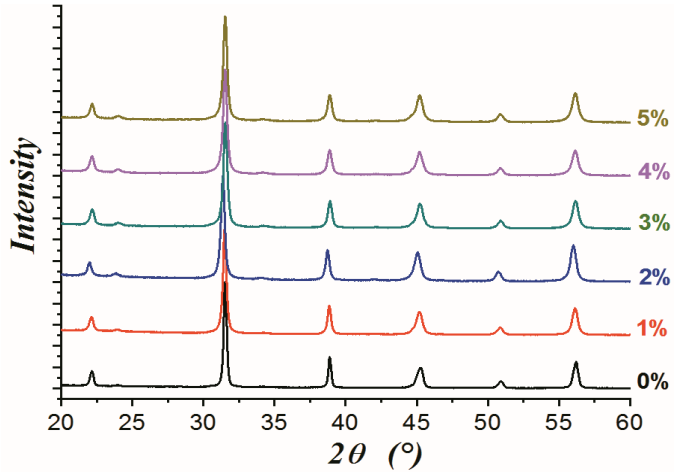

Figure 4. XRD patterns of BGT powders calcined at 950 °C 4h

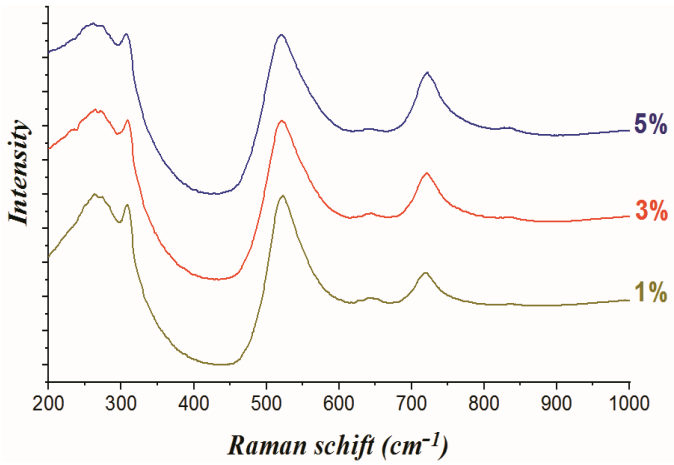

Figure 5. Room temperature Raman spectroscopy for BGT powders calcined at 950 °C (4h)

Fig.5. shows the Raman spectra for $BaTiO_3$ doped with several Gd concentrations prepared by the sol gel method. The graphs show the characteristic Raman peaks at room temperature of BGT located at 250 cm^{-1} (A1(TO)), 305 cm^{-1} [B1, E(LO+TO)] , 520 cm^{-1} [A1(TO), E(TO)]; 715 cm^{-1} [A1(LO3), E(LO)]. The extra band with a low intensity at 830 cm^{-1} is probably relative to Gd concentration [22]. This high- frequency mode (above 700 cm^{-1}) can be caused by the

vibrations resulting from the shift of oxygen and also correlated to the presence of oxygen vacancies [22]. Table.3 shows the evolution of the peak intensity of the Raman modes as a function of the composition of BGT powders. The Raman peak around 305 cm^{-1} showed a decrease in intensity by increasing the Gd concentration. As the crystalline structure of the undoped samples was not affected under doping with Gd, the intensity of this mode cannot in reality be sufficient to reflect its effect on the tetragonality and the formation of the phase structure as reported by some [11, 20]. However, we can observe from this table the influence of the incorporation of the gadolinium on frequencies and on FWHM of A1(LO3); A1(TO3); E(TO+LO) and E(TO), E(LO) Raman modes. The A1(LO3) mode position undergoes a continuous growth, which highlights the incorporation of Gd in the B site of the perovskite structure. For A1(TO3) mode, we notice an increase in the frequency from 520 cm^{-1} for the undoped BT to 521 cm^{-1} for BGT1% followed by a continuous decrease. So, we can conclude that Gd enters the two sites (Ba and Ti sites). This result agrees with those of XRD analysis (Fig.4 and Table 2).

Table 3. ***Intensity of the Raman modes as a function of the composition of BGT powders calcined at 950 °C for 4h***

Composition	**0%**	**1%**	**3%**	**5%**
A1(LO3), E(LO) mode position (cm^{-1})	715,59	719,45	720,41	721,37
FWHM of A1(LO3), E(LO) mode (cm^{-1})	34,80	36,60	48,46	54,25
A1(TO3) mode (cm^{-1})	520,81	521,78	520,81	519,85
FWHM of A1(TO3) mode (cm^{-1})	110,91	115,01	117,44	112,25
E(TO+LO) mode position (cm^{-1})	305,79	308,68	308,68	306,75
E(TO),E(LO)(cm^{-1})	186,22	188,15	192,97	192,01

Table 4. ***Intensity of [B1, E(LO,TO)] mode as a function of composition***

Samples	**0%**	**1%**	**3%**	**5%**
Intensity of E(LO+TO) mode at 305 cm^{-1}	17503,77	41211,85	38345,16	36644,80

3.2. ***Part2: Elaboration of BT and BGT samples with distilled water as solvent***

To check the effect of acetic acid on the crystal structure, we have prepared a series of pure and Gd-doped BT samples without adding this acid to the Ba^{2+} and Gd^{2+} solutions, by following the same experimental steps detailed in Part1. Fig.6 shows XRD patterns of the undoped BT powders calcined at 600 °C (8h), 850 °C (8h), 900 °C (8h), 950 °C (4h) and 1000 °C (4h). This Figure reveals the formation of the crystalline phase of the pure $BaTiO_3$ at 850 °C but with a secondary phase of $BaCO_3$. When the sample was fired at 900 °C and at 950 °C the intensity of the peak of the impurity phase (barium carbonate) decreased and the patterns showed a fully crystallized pseudo cubic perovskite structure. At 1000 °C, we observed a peak splitting around $2\theta = 45°$ which is due to the tetragonal phase [11,20].This result agrees with some literature reports indicating that the cubic phase of $BaTiO_3$ can be transformed to the tetragonal phase at 1000 °C [20]. Consequently, the effect of the acetic acid seems to play a more or less important role in the structure of BT material.

From Fig.1 and Fig.6, we can say that the use of acid acetic as solvent for barium acetate does not favor the tetragonal phase. Moreover, comparison of the spectra given in Figs.1 and 6 indicates that acetic acid improves the crystallization

at lower temperatures of the fine powders. Fig.7 displays XRD diffractograms of Gd doped BT samples recorded at room temperature. These spectra reveal a crystallization of the powders in the perovskite phase for all temperatures with the presence of some traces of secondary phase, and the intensity of the peaks relative to the impurity is almost constant under incorporation of Gd, which means that no correlation exists consecutive to an increase of the concentration of Gd. In addition, as we have been working in a high region of temperature and knowing that barium and titanium oxides persist at relatively high temperatures then these peaks could be attributed to $BaCO_3$. Moreover, the evolution of the diffractograms displayed in Fig. 7 indicates the presence of the tetragonal structure for all the concentrations and hence that up to 5% of doping the samples still not show a phase transition from tetragonal structure to pseudo cubic structure. This result is in agreement with those of the literature [22].

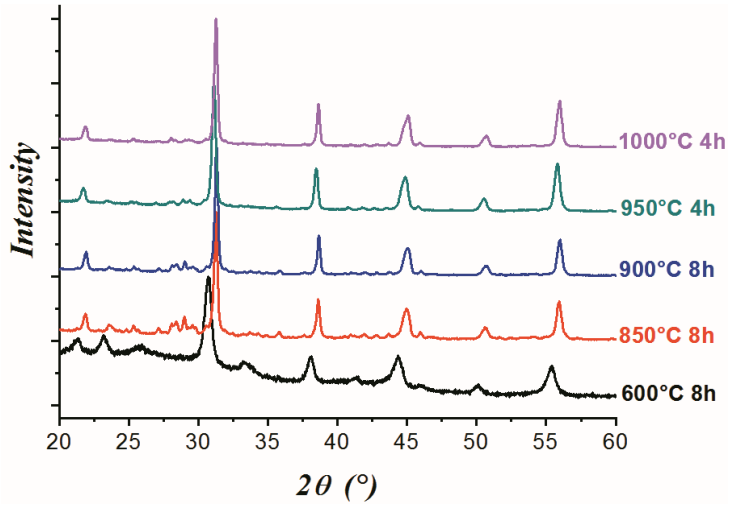

Figure 6. XRD patterns of $BaTiO_3$ powders calcined at different temperatures

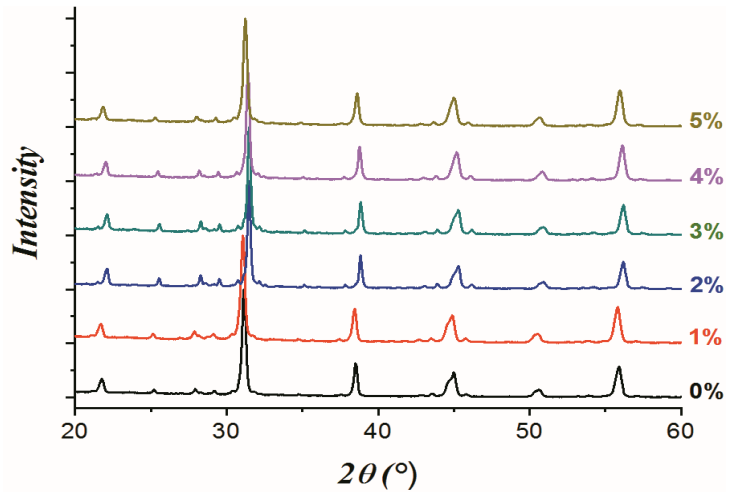

Figure 7. XRD patterns of BGT powders calcined at 1050 °C (4h)

We can then deduce that acetic acid influences the crystalline phase explaining the appearance of the stable pseudo-cubic phase in our samples (Part 1), together with its effect on the size of crystallites as shown in Fig.8. The size of crystallites shows an increase of about 4 nm for the undoped BT and a decrease for the doped samples. Here also, and as discussed above, the displacement of the peaks in the XRD spectra (Table. 5) shows that Gd ions may enter the two sites A and B. Fig.9 shows the Raman spectra, recorded at room temperature, of the BGT powder samples. It is known that in the tetragonal BT (P4mm) single crystal, the Raman modes are [A1(TO2)] mode at 266 cm^{-1}, a sharp peak

associated with [B1, E(LO,TO)] mode at 306 cm^{-1}, [A1(TO3)] mode at 516 cm^{-1} and [A1(LO3), E(LO)] mode at 720 cm^{-1} [24-25]. In the case of BGT samples, it can be noticed the existence of some differences between Raman spectra recorded at room temperature in Part 1 of the present work with those obtained in this part and also with the results from the literature.

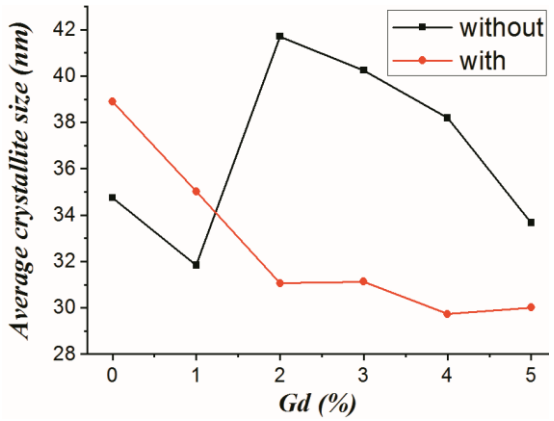

Figure 8. Average crystallite size of BGT powders calcined at 1050 °C during 4h

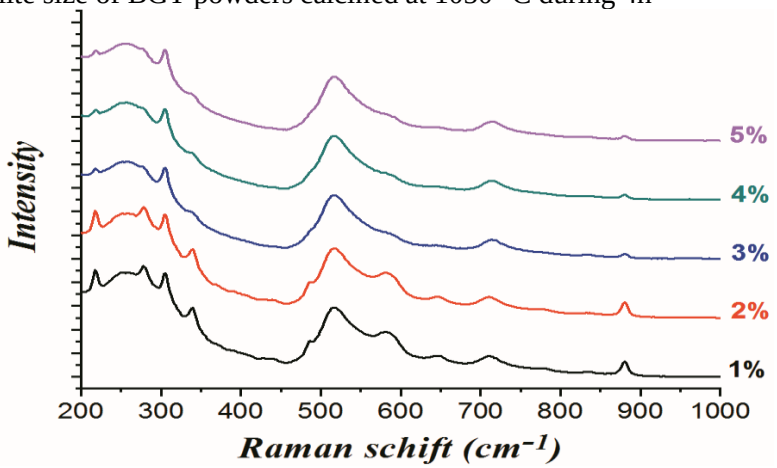

Figure 9. Room temperature Raman spectroscopy for BGT powders calcined at 1050 °C (4h)

Table 5. ***The average crystallite size; the position of the (111)-Peak; lattice parameters (a, c); tetragonality and volume of lattice of BGT***

Samples	A. c. s.(nm)	P. of the (111)-P.	c(Å)	a(Å)	c/a	V(Å³)
0%	34.75	31,1433	4.100	4.020	1.0199	66.25764
1%	31.84	31,0583	4.060	4.020	1.0099	65.61122
2%	41.71	31,4663	4.030	3.990	1.0100	64.15800
3%	40.25	31,4833	4.010	3.999	1.0027	64.12792
4%	38.19	31,4153	4.020	3.999	1.0052	64.28784
5%	33.67	31,2283	4.040	4.010	1.0074	64.96360

Table 6. ***Intensity of [B1, E(LO,TO)] mode as function of composition***

Sample	1%	2%	3%	4%	5%
Intensity of E(LO+TO) mode at 305 cm^{-1}	18347,1	18347,1	6672,86	6672,86	6672,86

First of all, we noticed the overlap of several modes (Fig. 9) also observed between 200 and 280 cm^{-1} and around 500 cm^{-1} and 700 cm^{-1} in different works published before, but on the other hand all the active Raman modes relative to the BT structure are present which allows to say that these results are very special and unique in terms of information on details of the tetragonal structure of BT. For the BGT1% sample, it especially shows the appearance of the following Raman modes: 216 cm^{-1}; 253 cm^{-1}; 278 cm^{-1}; 305 cm^{-1}; 340 cm^{-1}; 488 cm^{-1}; 519 cm^{-1}; 581 cm^{-1}; 644 cm^{-1}; 714 cm^{-1}. These additional modes gradually disappear from the BGT1% spectrum as the concentration of Gd increases as a consequence of an overlapping which leads to intense broad and asymmetric bands. The BGT5% sample shows the traditional quadratic phase as all the Raman modes associated with this phase are present which confirms the result of the XRD (no appearance of a phase transition). As shown in Table 6 the intensity of E(LO+TO) Raman mode stay almost constant. These results confirm again the effect of acetic acid on the crystalline phase.

Conclusion

From the present study, we can infer that acetic acid provokes the formation of the stable pseudo-cubic structure until a temperature of the order of 1000 °C, for the undoped and for doped samples at low values of crystallization temperature in comparison with the samples elaborated without the use of acetic acid. A phase transition was not yet observed in this range ($0.00 \leq x \leq 0.05$). The Gd element may replace the Ti and the Ba elements.

References

[1] F. Valdivieso, M. Pijolat and M. Soustelle, « Étude cinétique d'une voie de synthèse du titanate de baryum à partir de réactifs (nitrate de baryum et dioxyde de titane) à l'état solide», *J. Chim. Phys.*, 94 (1997) 159-180.

[2] S. Nenez, « Céramiques diélectriques commandables pour applications micro-ondes : composites à base de titanate de baryum-strontium et d'un oxyde non ferroélectrique », *Thèse de Doctorat, Université de Bourgogne, UFR Sciences et Techniques, Laboratoire de Recherches sur la Réactivité des Solides, UMR 5613 – CNRS,* (2001).

[3] M. Mesrar, T. Lamcharfi, N. S. Echatoui, F. Abdi, F. Z. Ahjyaje and M. Haddad, "Effect of barium doping on electrical and electromechanical properties of $(1-x)(Na_{0.5}Bi_{0.5})TiO_3$-$xBaTiO_3$", *Mediterranean Journal of Chemistry*, 8 (2) (2019) 198-208.

[4] F. Z. FADIL, « Synthèse et caractérisation des matériaux PT: Mg et LN : Mg /Ho en vue de fabrication de fibres cristallines », *Thèse de doctorat, Facultés des Sciences et Techniques de Fès, Maroc,* (2012).

[5] C. Chen, H. Hao, T. Wang, J. Cheng, Z. Luo, L. Zhang, M. Cao, Z. Yao, H. Liu, "Nano-$BaTiO_3$ phase transition behavior in coated $BaTiO_3$-based dielectric ceramics", *Ceramics International*, 45 (6) (2019) 7166-7172.
https://doi.org/10.1016/j.ceramint.2018.12.223

[6] M. H. Frey and D. A. Payne, "Grain-size effect on structure and phase transformations for barium titanate", *Phys. Rev. B,* 54 (1996) 3158.

[7] W. Bąk, C. Kajtoch, S. Ptaszek, A. Lisińska-Czekaj, D. Czekaj, D. Ziętek, T. Glos, B. Garbarz-Glos, "Influence of Sn and Pb ions substitutions on dielectric properties of barium titanate", *Arch. Metall. Mater.*, 61 (2) (2016) 905-908.
DOI: 10.1515/amm-2016-0153

[8] A. J. Priyanka and A. K. Jha, "Effect of holmium substitution on structural and electrical properties of barium zirconate titanate ferroelectric ceramics", *Ceramics International*, 40 (4) (2014) 5209-5216.

[9] K. Matsuura, T. Hoshina, H. Takeda, Y. Sakabe and T. Tsurumi, "Effects of Ca substitution on room temperature resistivity of donor-doped barium titanate based PTCR ceramics", *Journal of the Ceramic Society of Japan,* 122 (6) (2014) 402-405.
[10] M. S. Alkathy, R. Gayam and K.C. J. Raju, "Effect of nickel and lithium co-substituted Barium titanate ceramics on structural and dielectric properties", *Journal of Materials Science: Materials in Electronic*, 28 (2017) 1684-1694.
[11] A. Elbasset, « Synthèse et caractérisation de matériaux de titanate de baryum purs et dopés au strontium et au zirconium », *Thèse de doctorat, Facultés des Sciences et Techniques de Fès, Maroc,* (2014).
[12] H. Serajul , H. A. Akhtar, K. B. Prem., "Effect of casting process parameters of Al6061-Cu- SiCp metal matrix composite on material removal rate by electrical discharge machining ", *Mor. J. Chem*., 2 (4) (2014) 343-349.
[13] A. V. Rane, V. K. Abitha, M. R. Niji, K. Rajkumar, P.S. Suchithra, "Mechanical, thermal, X-Ray diffraction studies in nanocomposites based on thermoplastic polyurethanes and nanosilica for radiation resistance", *Mor. J. Chem*., 3 (3) (2015) 540-549.
[14] N. Dighore, S. Dhonde, S. Gaikwad, A. Rajbhoj, *"Synthesis of conducting polymer Polypyrrole-MoO_3 nanocomposites", Mor. J. Chem*., 4 (3) (2016) 797-804.
[15] A. Zyane, A. Belfkira, F. Brouillette, R. Lucas, P. Marchet, « Substitution de $BaTiO_3$ dans les composites diélectriques par un matériau vert, écologique et économique », *Colloque Annuel du CQMF, Shawinigan*, (2013).
[16] F. S. Yen, H. Hsiang and Y. Chang, "Cubic to tetragonal phase transformation of ultrafine $BaTiO_3$ crystallites at room temperature", *Jpn. J. Appl. Phys.,* 34 (1995) 6149-6155.
[17] B. lee and J. Zhang, "preparation, structure evolution and dielectric properties of $BaTiO_3$ thin films and powders by an aqueous sol-gel process", *thin solid films,* 388 (2001) 107-113.
[18] W. Li, Z. Xu , R. Chu, P. Fu and J. Hao, "structure and electrical properties of $BaTiO_3$ prepared by sol gel process", *journal of alloys and compounds*, 482 (2009) 137-140.
[19] X. Li and W. H. Shih, "Size effects in barium titanate particles and clusters", *J. Am. Cerami. Soc.*, 80 (11) (1997) 2844-2852.
[20] A. Salhi, S. Sayouri, B. Jaber, L. Omari, "Effect of microwaves on the synthesis, structural and dielectric properties of Ca-modified $BaTiO_3$ ceramics", *Applied Physics A: Materials Science and Processing*, 124 (2018) 389.
[21] F. Es-saddik, K. Limame, S. Sayouri, T. Lamcharfi, "Effect of the occupation of Ba and Ti sites on the structural, optical and dielectric properties of Sm-doped $BaTiO_3$ ceramics", *Journal of Materials Science: Materials in Electronics*, 30 (2019) 1821-1831.
[22] J. P. Hernandez lara and al., "structural evolution and electrical properties of $BaTiO_3$ doped with Gd", *Materials Research*, 20 (2) (2017) 538-542.
[23] M. Belhajji, S. Sayouri, A. Nfissi and T. Lamcharfi, "Effect of the occupation of Pb and Ti sites on the structural, microstructural and dielectric properties of Y-doped $PbTiO_3$ samples", *Journal of Materials Science: Materials in Electronics*, 30 (12) (2019).
https://doi.org/10.1007/s10854-019-01977-8
[24] A. Pinczuk, W. Taylor, E. Burstein, I. Lefkowitz, "The Raman spectrum of $BaTiO_3$", *Solid State Communications*, 5 (5) (1967) 429-433.
[25] C. H. Perry and D. B. Hall, "Temperature dependence of the Raman spectrum of $BaTiO_3$", *Physical review letters*, 15 (17) (1965).